AMERICAN SOCIETY FOR MICROBIOLOGY | Applied and Environmental Microbiology

Activity-Based Protein Profiling of Ammonia Monooxygenase in *Nitrosomonas europaea*

Kristen Bennett,[a] Natalie C. Sadler,[b] Aaron T. Wright,[b] Chris Yeager,[c] Michael R. Hyman[a]

Department of Plant and Microbial Biology, North Carolina State University, Raleigh, North Carolina, USA[a]; Biological Sciences Division, Pacific Northwest National Laboratory, Richland, Washington, USA[b]; Biosciences Division, Los Alamos National Laboratory, Los Alamos, New Mexico, USA[c]

Nitrosomonas europaea **is an aerobic nitrifying bacterium that oxidizes ammonia (NH_3) to nitrite (NO_2^-) through the sequential activities of ammonia monooxygenase (AMO) and hydroxylamine dehydrogenase (HAO). Many alkynes are mechanism-based inactivators of AMO, and here we describe an activity-based protein profiling method for this enzyme using 1,7-octadiyne (17OD) as a probe. Inactivation of NH_4^+-dependent O_2 uptake by *N. europaea* by 17OD was time- and concentration-dependent. The effects of 17OD were specific for ammonia-oxidizing activity, and *de novo* protein synthesis was required to reestablish this activity after cells were exposed to 17OD. Cells were reacted with Alexa Fluor 647 azide using a copper-catalyzed azide-alkyne cycloaddition (CuAAC) (click) reaction, solubilized, and analyzed by SDS-PAGE and infrared (IR) scanning. A fluorescent 28-kDa polypeptide was observed for cells previously exposed to 17OD but not for cells treated with either allylthiourea or acetylene prior to exposure to 17OD or for cells not previously exposed to 17OD. The fluorescent polypeptide was membrane associated and aggregated when heated with β-mercaptoethanol and SDS. The fluorescent polypeptide was also detected in cells pretreated with other diynes, but not in cells pretreated with structural homologs containing a single ethynyl functional group. The membrane fraction from 17OD-treated cells was conjugated with biotin-azide and solubilized in SDS. Streptavidin affinity-purified polypeptides were on-bead trypsin-digested, and amino acid sequences of the peptide fragments were determined by liquid chromatography-mass spectrometry (LC-MS) analysis. Peptide fragments from AmoA were the predominant peptides detected in 17OD-treated samples. In-gel digestion and matrix-assisted laser desorption ionization–tandem time of flight (MALDI-TOF/TOF) analyses also confirmed that the fluorescent 28-kDa polypeptide was AmoA.**

Activity-based protein profiling (ABPP) is a well-established proteomics method used to identify catalytically active enzymes in complex mixtures (1, 2). Although many variations exist, ABPP often involves the use of bifunctional enzyme probes. One group enables the probe to act as a mechanism-based inactivator. Activation of this functional group by the target enzyme results in covalent modification and inactivation of the enzyme by the probe (Fig. 1A). The probe's second functional group is often either an ethynyl or azide group that can then be reacted with a complementary azide- or ethynyl-containing reporter molecule using a copper-catalyzed azide-alkyne cycloaddition (CuAAC) reaction (1, 3) (Fig. 1B). Depending on the reporter molecule used, the inactive enzyme-probe-reporter conjugate can then be visualized in SDS-PAGE or affinity purified, proteolytically digested, and then identified after analysis of the resulting peptide fragments by mass spectrometry. This type of ABPP has been used to study mammalian cytochrome P450s (4) and several classes of bacterial enzymes (3) but has not been previously applied to bacterial monooxygenases.

In this study, we have characterized 1,7-octadiyne (17OD) and various other diynes as ABPP probes for ammonia monooxygenase (AMO) in the ammonia-oxidizing bacterium (AOB) *Nitrosomonas europaea*. This chemolithoautotroph obtains energy for CO_2 fixation and growth from oxidizing ammonia (NH_3) to nitrite (NO_2^-) (5). The initial oxidation of ammonia is catalyzed by membrane-bound AMO while hydroxylamine (NH_2OH), the immediate product of ammonia oxidation, is further oxidized to nitrite (NO_2^-) by the periplasmic enzyme hydroxylamine dehydrogenase (HAO) (5). Although *N. europaea* is the most extensively studied AOB, studies of AMO in this bacterium and AOB in general have historically been hampered by the labile nature of this enzyme (6–8). However, even though AMO has not yet been obtained in a highly purified active state, considerable insights into the activities and structure of this important enzyme have been obtained from whole-cell studies of *N. europaea* using different classes of inhibitors (5, 9). For example, ammonia oxidation is often strongly but reversibly inhibited by metal-binding agents, and some of the most potent of these are copper-selective compounds such as allylthiourea (9). The selectivity of these compounds for copper as well as the fact that AMO activity can be stimulated and stabilized by copper ions in cell extracts (6, 7) suggests that AMO is a copper-dependent enzyme. Many organic compounds also reversibly inhibit ammonia oxidation through their action as alternative substrates for AMO. These compounds include diverse alkanes (10, 11), alkenes (11, 12), aromatics (13, 14), ethers (15, 16), and halogenated compounds (15, 17, 18). The simplest organic AMO substrates, such as methane and ethylene, are competitive inhibitors of ammonia oxidation (10, 12), while other substrates exhibit more complex inhibition patterns (19).

Received 1 November 2015 **Accepted** 27 January 2016

Accepted manuscript posted online 29 January 2016

Citation Bennett K, Sadler NC, Wright AT, Yeager C, Hyman MR. 2016. Activity-based protein profiling of ammonia monooxygenase in *Nitrosomonas europaea*. Appl Environ Microbiol 82:2270–2279. doi:10.1128/AEM.03556-15.

Editor: F. E. Löffler, University of Tennessee and Oak Ridge National Laboratory

Address correspondence to Michael R. Hyman, mrhyman@ncsu.edu.

Supplemental material for this article may be found at http://dx.doi.org/10.1128/AEM.03556-15.

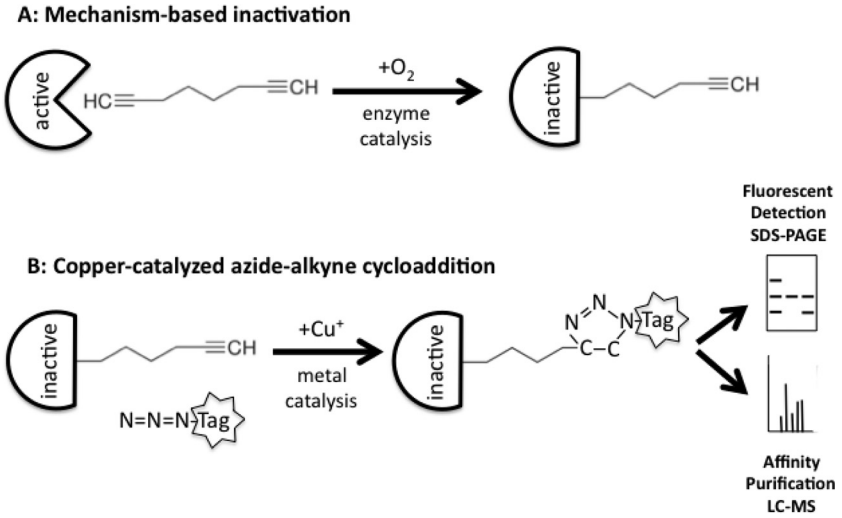

FIG 1 Schematic of the activity-based protein profiling (ABPP) method for detection of ammonia monooxygenase (AMO). (A) Mechanism-based inactivation. Catalytic activation of one terminal ethynyl group of the symmetrical diyne probe by AMO leads to the formation of a reactive intermediate (most likely a ketene). The reactive group forms a covalent bond with AMO, resulting in a catalytically inactive, enzyme-inactivator adduct. Critically, the terminus of the diyne probe that was not activated (and covalently attached) to AMO retains an unreacted ethynyl group. (B) Copper-catalyzed azide/alkyne cycloaddition. The free ethynyl group of the inactive enzyme-inactivator adduct is conjugated with either a visualization tag (e.g., Alexa Fluor 647 azide) or an affinity purification tag (e.g., biotin-azide) using a copper-catalyzed azide-alkyne cycloaddition (CuAAC) reaction. The resulting enzyme-probe-tag conjugant can then either be (i) visualized using IR fluorescence in SDS-PAGE or (ii) enriched by affinity chromatograph, tryptically digested, and identified by LC-MS/MS.

Insights into the structure of AMO have more often come from studies of irreversible inactivators than from those of reversible inhibitors of this enzyme. Recognized AMO inactivators include terminal and subterminal alkynes (9, 11, 20, 21), allyl sulfide (22), and some aniline and cyclopropane derivatives (21). These compounds are thought to be catalytically activated by AMO to reactive intermediates that subsequently covalently bind to and irreversibly inactivate the enzyme. The canonical mechanism-based inactivator of AMO is acetylene (C_2H_2). The potent and specific effects of acetylene on ammonia oxidation by *N. europaea* were first recognized by Hynes and Knowles (23, 24). A subsequent kinetic study (20) demonstrated that the effects of acetylene conform to many of the well-established criteria for mechanism-based inactivation (25). For example, the effects of acetylene on NH_4^+-dependent O_2 uptake are time and concentration dependent, and AMO activity is not inactivated by acetylene under anoxic conditions when AMO is catalytically inactive (20). The effects of acetylene are also irreversible, and cells require *de novo* protein synthesis to reestablish AMO activity after exposure to this gas (26). Incubation of *N. europaea* with $^{14}C_2H_2$ leads to the covalent radiolabeling of a membrane-associated 28-kDa polypeptide (20, 26), and this radiolabeling is prevented if cells are exposed to a reversible inhibitor, such as thiourea, during exposure to $^{14}C_2H_2$ (20). Based on this series of observations, the ^{14}C-labeled 28-kDa polypeptide was proposed to be a structural component of AMO (20). The binding of ^{14}C from $^{14}C_2H_2$ on the 28-kDa polypeptide is compatible with covalent attachment of a ketene to amino acid H191, which is thought to reside in, or nearby, the active site of AMO (27). The 28-kDa polypeptide in *N. europaea* has also been labeled *in vivo* with a fluorescent derivative of propargylamine (prop-2-yn-1-amine), and the N-terminal amino acid sequence of the polypeptide was used to identify its corresponding gene (*amoA*) (28). Like several other genes encoding key enzymes involved in ammonia oxidation in *N. europaea*, identical copies of *amoA* occur in multiple operons (*amoCAB*) (5, 29), and expression of these *amoA* copies cannot be discriminated at the translational level. AmoA also has a predicted mass of ~32 kDa rather than 28 kDa (29). This suggests that AmoA migrates aberrantly in SDS-PAGE systems, and, like other intrinsic membrane proteins (30, 31), AmoA aggregates in SDS-PAGE sample buffer if heated at high temperature (95°C) in the presence of β-mercaptoethanol (32).

Covalent modification of structural proteins, a definitive feature of mechanism-based inactivation, has not been confirmed for putative AMO inactivators other than acetylene and propargylamine. This likely reflects the limited commercial availability and high cost of suitably radiolabeled forms of these compounds. In this study, we have characterized 17OD as a mechanism-based inactivator of AMO, and we have shown that after inactivation, AmoA can be specifically labeled using CuAAC reactions with azide-containing reporter molecules that can then be used to either detect or selectively purify this polypeptide. Our results are discussed in terms of the advantages and disadvantages of using ABPP for studying different AMOs and the potential applicability of this approach to other alkyne-sensitive bacterial monooxygenases in pure culture studies and environmental samples.

MATERIALS AND METHODS

Materials. *N. europaea* (ATCC 19178) was obtained from the American Type Culture Collection (Manassas, VA). Alexa Fluor 647 azide (99% purity) was obtained from Invitrogen (Grand Island, NY). Aminoguanidine hydrochloride (≥98% purity), 1-allyl-2-thiourea (98% purity), bovine serum albumin, 3-butyn-1-ol (97% purity), 1,4-diethynylbenzene (96% purity), dipropargylamine (97% purity), 1-hexyne (97% purity), hydroxylamine hydrochloride (>99.99% purity), *N*-(1-naphthyl)ethylenediamine dihydrochloride (98% purity), 1,7-octadiyne (17OD; 98% purity), phenylacetylene (98% purity), propargylamine (98% purity), sulfanilamide (>99% purity), and Tris-(3-hydroxypropyltriazolylmethyl) amine (THPTA; 95% purity) were obtained from Sigma-Aldrich Co.

(Milwaukee, WI). *N*-(3-Azidopropyl)biotinamide (biotin-azide) (95% purity), 1-heptyne (98% purity), 1,6-heptadiyne (97% purity), 1-octyne (97% purity), 1-nonyne (99% purity), and 1,8-nonadiyne (>95% purity) were obtained from TCI America (Portland, OR). 1,5-Hexadiyne (50%, vol/vol, in pentane) was obtained from Alfa Aesar (Ward Hill, MA). Streptavidin agarose (6% beaded agarose slurried in water) and Tris-(2-carboxyethyl)phosphine hydrochloride (TCEP) (≥98% purity) were obtained from Thermo Fisher Scientific (Grand Island, NY). Tris-[(1-benzyl-1H-1,2,3-triazol-4-yl)methyl]amine (TBTA) (97% purity) was obtained from AnaSpec (Fremont, CA).

Growth and harvesting of bacteria. Cells of *N. europaea* were grown in batch culture in mineral salts medium containing $(NH_4)_2SO_4$ (25 mM), harvested, and finally resuspended at ~0.2 g wet weight ml^{-1} in buffer (50 mM sodium phosphate, pH 7.8, plus 2 mM $MgCl_2$) as described previously (26). Unless otherwise stated, this buffer was used throughout the experiments described in this study.

Oxygen uptake measurements. All measurements of O_2 uptake were made using a Clark-style oxygen electrode (Hansatech, King's Lynn, Norfolk, United Kingdom) operated at 30°C. The reaction chamber contained buffer (2 ml), and in a typical reaction, a basal rate of O_2 uptake in the absence of cells was established for 2 to 3 min. Substrates and inactivators (≤10 μl) were then added to the electrode chamber from concentrated stock solutions using microsyringes inserted through the capillary aperture in the screw-top seal of the reaction chamber. The reactions were then initiated by the addition of cells (50 μl; ~100 μg total protein), and the time course of O_2 uptake was monitored using a chart recorder. The rates of inactivation of NH_4^+-dependent O_2 uptake by 17OD were determined by measuring the slope of the recorded O_2 uptake reactions at 30-s intervals after the addition of cells. The activity at each time point was then compared to the rate of O_2 uptake at the same time point for reactions conducted in the absence of 17OD. The differences between the slopes of the O_2 uptake reactions at each time point were then expressed as percentages of activity remaining.

Inactivation of ammonia-oxidizing activity of resting cells by 17OD and other alkynes. The ammonia-oxidizing activity of *N. europaea* was routinely inactivated by 17OD in reactions conducted in glass serum vials (60 ml). The reaction vials initially contained buffer (~19 ml) and were sealed with butyl rubber stoppers and aluminum crimp seals (Wheaton Scientific, Millville, NJ). NH_4Cl (200 μmol) was added from a concentrated aqueous stock solution (1 M), and 17OD (20 μmol) was added from concentrated stock solution (1.0 M) in dimethyl sulfoxide (DMSO). The reaction was initiated by the addition of a concentrated cell suspension (1 ml) to give a final reaction mixture volume of 20 ml. The reaction vials were incubated for 1 h at 30°C in a shaking water bath operated at 150 rpm. Untreated control cells were incubated as described above, except that DMSO alone (20 μl) was added to the reaction mixture rather than 17OD in DMSO. After 1 h, a sample (4 μl) was withdrawn from the reaction medium to colorimetrically determine the amount of NO_2^- that had been generated during incubation (33). In all cases, 17OD-treated cells had NH_4^+-dependent NO_2^--generating activities that were ≤1% of the activity of untreated control cells. The cells were then harvested from these reaction mixtures by centrifugation (10,000 × *g* for 2 min), and the resulting cell pellets were resuspended in buffer (15 ml). This washing procedure was repeated 3 times. After the final centrifugation, the cell pellets were resuspended in buffer (1 ml) and were stored at 4°C for ≤2 h prior to use in experiments.

Cells were also treated with 17OD in the presence and absence of allylthiourea or acetylene. These incubations were conducted in glass serum vials (10 ml) that contained buffer (750 μl) and allylthiourea (100 nmol) added from a stock solution in DMSO (0.1 M), DMSO alone (1 μl), or acetylene (1%, vol/vol, gas phase). The reactions were initiated by the addition of cells (250 μl, ~25 mg total protein), and the vials were then incubated at 30°C in a shaking water bath operated at 150 rpm. After 10 min, the reaction mixtures were all supplemented with NH_4Cl (10 μmol) that was added from an aqueous stock solution (1 M); 17OD (1 μmol) was also added as a stock solution in DMSO (1 M) as needed. The reaction vials were then incubated for a further 10 min at 30°C. The cells were then harvested from these reaction mixtures by centrifugation using a microcentrifuge (10,000 × *g* for 2 min). The resulting cell pellets were then resuspended in 2× SDS-PAGE sample buffer (250 μl) that contained 0.125 M Tris (pH 6.8), 4% SDS, 20% glycerol, 10% β-mercaptoethanol, and 0.002% bromophenol blue. The solubilized cell extracts were subsequently conjugated with Alexa Fluor 647 azide in a CuAAC reaction as described below.

Cells were also treated with other *n*-alkynes and diynes in small-scale reactions conducted in glass serum vials (10 ml) that were sealed with butyl rubber stoppers and aluminum crimp seals. The reaction medium contained buffer (~750 μl) and NH_4Cl (10 μmol) added from a concentrated aqueous stock solution (1 M). The reaction mixtures also contained individual alkynes or diynes (1 μmol) added from stock solutions in DMSO (1 M). For untreated control cells, the reaction medium contained NH_4Cl (10 μmol) and DMSO (1 μl). The reactions were initiated by the addition of resting cells (250 μl; ~25 mg total protein) to give a final reaction mixture volume of 1 ml. The vials were then incubated at 30°C in a shaking water bath operated at 150 rpm. After 1 h, a sample (4 μl) was withdrawn from the reaction mixtures to determine the amount of NO_2^- that had been generated (33). The cells were then recovered from the remainder of the reaction medium by centrifugation (10,000 × *g* for 2 min), and the cell pellet was resuspended in buffer (1 ml). This procedure was repeated 3 times, and the final cell pellet was resuspended in buffer (300 μl). A portion of these cells (150 μg total protein) was subjected to CuAAC reactions with Alexa Fluor 647 azide as described below.

Effect of NH_4^+ concentration on the inactivation of NH_4^+-dependent NO_2^- production by 17OD. The reactions were conducted in glass serum vials (10 ml) that were sealed with butyl rubber stoppers and aluminum seals. The reaction vials contained buffer (450 μl), various concentrations of NH_4Cl (0, 0.5, 1.0, 2.5, 5.0, or 10 mM) added from an aqueous stock solution (1 M), and a fixed amount of 17OD (0.5 μmol) added from a stock solution in DMSO (1 M). The reactions were initiated with the addition of cells (50 μl, ~0.5 mg total protein), and the reaction vials were incubated at 30°C in a shaking water bath operated at 150 rpm. After incubation for 15 min, cells were recovered from the medium by centrifugation (10,000 × *g* for 2 min), and the resulting cell pellet was then resuspended in buffer (1 ml). This procedure was repeated 3 times, and the final cell pellet was resuspended in buffer (300 μl). The washed cells were then added to glass serum vials (10 ml) that contained buffer (700 μl) and NH_4Cl (10 μmol) that was added from a concentrated aqueous stock solution (1 M). The vials were sealed with butyl rubber stoppers and aluminum seals and were then incubated at 30°C in a shaking water bath operated at 150 rpm. After incubation for 15 min, acetylene (1 ml) was then added to the gas phase to inhibit further NH_4^+-dependent NO_2^- production. Samples (4 μl) were then withdrawn from each vial to colorimetrically determine the concentration of NO_2^- (33).

Recovery of NH_4^+-dependent NO_2^--generating activity after exposure to 17OD. Resting cells were treated with 17OD (1 μmol) in the presence of NH_4Cl (10 mM) and were then harvested and washed as described above. Untreated control cells were similarly treated, except neat DMSO was added to the reaction mixtures instead of 17OD dissolved in DMSO. The treated, washed cells (~15 mg total protein) were then added to glass serum vials (60 ml) that contained growth medium (~9.7 ml) (26) supplemented with either rifampin (100 μg ml^{-1}) or chloramphenicol (400 μg ml^{-1}) as required to give a final reaction mixture volume of 10 ml. The reaction vials were then incubated at 30°C in a shaking water bath operated at 150 rpm. Samples of the reaction mixtures (4 μl) were removed at intervals to determine the amount of NO_2^- generated from ammonia oxidation.

CuAAC reaction conditions. Unless otherwise stated, CuAAC reactions were conducted using whole cells of *N. europaea* that were incubated in plastic microcentrifuge tubes (500 μl) in a final reaction mixture volume of 75 μl. The concentrations of reactants and times of incubation

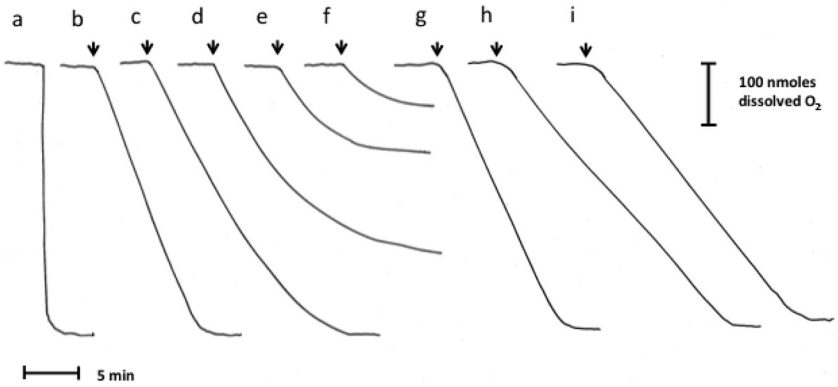

FIG 2 Time courses of O_2 uptake were determined in an O_2 electrode apparatus as described in the Materials and Methods section. Trace a shows the time course for chemical reduction of dissolved O_2 with sodium dithionite. The traces b to g show the reaction time courses for *N. europaea* incubated with 10 mM NH_4Cl and the following concentrations of 17OD added from a stock solution in DMSO: (b) 0 μM, (c) 1.25 μM, (d) 2.5 μM, (e) 5 μM, (f) 10 μM, and (g) neat DMSO (4 μl). The traces h and i were for *N. europaea* incubated with 1 mM $NH_2OH{\cdot}HCl$ with either neat DMSO (20 μl) (h) or 50 μM 17OD (i) added from a stock solution in DMSO. In each case, the arrows indicate the point at which cells were added to the electrode chamber to initiate the reactions.

used in these reaction mixtures were based on experiments using whole cells (see Fig. S1A, S2A, S3A, and S4A in the supplemental material) and frozen, lysed cells (see Fig. S1B, S2B, S3B, and S4B in the supplemental material) as reported in the supplemental material. In a typical reaction, whole cells in buffer (150 μg total protein) were mixed with Alexa Fluor 647 azide (16 μM final concentration) that was added from a stock solution (0.6 mM) in DMSO. The reactions were initiated by the addition of $CuSO_4$ (2 mM final concentration) and sodium ascorbate (11 mM final concentration) that was added from freshly prepared aqueous stock solutions. Distilled water was added as required to obtain a final reaction mixture volume of 75 μl. In some reactions, either THPTA (1 mM) or aminoguanidine hydrochloride (1 mM) was also added to the reaction mixtures from concentrated aqueous stock solutions. Unless otherwise stated, the CuAAC reactions were conducted for 60 min at room temperature in darkness. The reactions were terminated by the addition of excess 3-butyn-1-ol (13 mM) that was added from an aqueous stock solution (1 M). Samples from the CuAAC reaction mixtures were then solubilized at room temperature by adding 2× SDS-PAGE sample buffer (75 μl). The solubilized cell samples were then centrifuged (10,000 × *g* for 2 min) to remove insoluble materials. The resulting supernatant was stored in the dark at −20°C prior to analysis by SDS-PAGE.

Cell fractionation. Cells were fractionated in soluble and particulate fractions by repeated freezing and thawing and subsequent centrifugation as described previously (20).

SDS-PAGE and IR scanning. Unless otherwise stated, SDS-PAGE analyses were conducted using precast 12% discontinuous SDS-polyacrylamide gels and a Bio-Rad Mini-Protean Tetra system (Bio-Rad Laboratories, Hercules, CA). Unless otherwise stated, samples contained ~25 μg total protein, and the gels were electrophoresed at room temperature for 30 min at a fixed current of 25 to 35 mA. To visualize fluorescently labeled polypeptides, the unfixed gel was immediately scanned with an excitation wavelength of 650 nm and a detection wavelength of 668 nm using an Odyssey 9120 infrared (IR) scanner (LI-COR Biosciences, Lincoln, NE). A near-infrared (NIR) marker protein ladder (Thermo Scientific, Waltham, MA) was used to estimate the mass of fluorescently labeled polypeptides.

Protein determination. Unless otherwise stated, the concentration of protein was determined with a biuret assay (34) after solubilization of cell material for 1 h at 65°C in 3 M NaOH and sedimentation of insoluble material by centrifugation (10,000 × *g* for 2 min). Bovine serum albumin was used as the standard.

RESULTS

Effect of 17OD on ammonia and hydroxylamine oxidation. The effects of 17OD on the ammonia- and hydroxylamine-oxidizing activities of *N. europaea* were determined by measurements of substrate-stimulated O_2 uptake. In the absence of 17OD, NH_4Cl stimulated a high rate of O_2 uptake that was effectively constant until the majority (>95%) of the dissolved O_2 had been consumed (Fig. 2, trace b). Low concentrations of 17OD (≤10 μM) produced a time-dependent loss of this NH_4^+-dependent O_2 uptake, and the rate of loss of activity increased with increases in 17OD concentration (Fig. 2, traces c to f). The effects of 17OD appeared to be specific for ammonia-oxidizing activity, as there was no inhibitory effect of 50 μM 17OD on the rate of hydroxylamine-dependent O_2 uptake (Fig. 2, traces h and i). Analyses of the rate of inactivation of NH_4^+-dependent O_2 uptake by 17OD using semilog plots of the percentage of O_2 uptake activity remaining versus time were linear and indicated the loss of activity was a first-order process for cells incubated with ≤10 μM 17OD (Fig. 3).

The potential for a protective effect of NH_4^+ on the rate of inactivation of ammonia-oxidizing activity was investigated by incubating cells with 17OD (1 μmol) and a range of initial NH_4Cl concentrations (0 to 10 mM). After incubation for 15 min, the cells were harvested from the reaction medium, washed with buffer, and assayed for residual NH_4^+-dependent NO_2^--generating activity. In all cases, the activity was fully inactivated (≥99%) after exposure to 17OD. Thus, NH_4Cl did not protect against inactivation of ammonia-oxidizing activity by 17OD under the conditions tested. This result further suggested that the effects of 17OD were irreversible.

To better characterize the irreversibility of the reaction, cells were incubated with NH_4Cl with and without 17OD, washed, and then incubated in fresh growth medium. Production of NO_2^- was then monitored over time in the presence and absence of protein synthesis inhibitors. Control cells that were not exposed to 17OD rapidly generated NO_2^- without a lag phase (Fig. 4). The rate of NO_2^- production by untreated cells was ~15% and ~30% lower in the presence of rifampin and chloramphenicol, respectively. For washed, 17OD-pretreated cells, the rate of NO_2^- production in fresh medium was close to zero over the first 1 h of the incubation. Over the subsequent 3 h, the rate of NO_2^- production progressively increased and after 4 h was nearly equivalent to the rate observed with control cells that had not been pretreated with 17OD. In contrast, the rate of NO_2^- production by 17OD-pre-

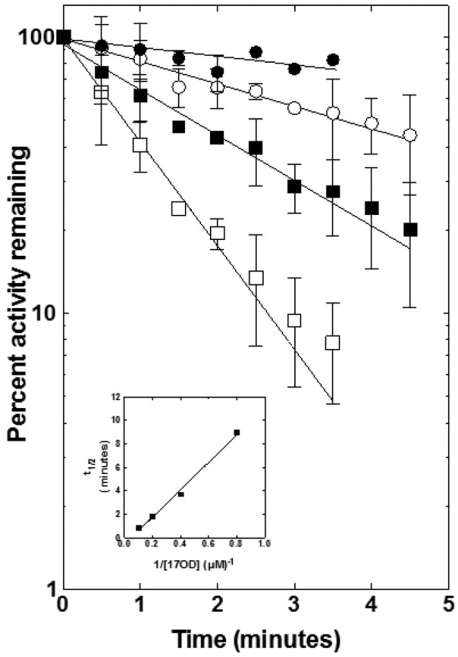

FIG 3 Semilog plots of the percentage of remaining NH_4^+-dependent O_2 uptake activity of *N. europaea* were determined for the reactions shown in Fig. 2 and two additional biological replicates, as described in the Materials and Methods section. Cells were incubated with 10 mM NH_4Cl and the following concentrations of 17OD: 1.25 μM (●), 2.5 μM (○), 5 μM (■), and 10 μM (□). The plots show the mean and standard error for the three biological replicates. The inset shows the extrapolated half-life of enzyme activity ($t_{1/2}$) plotted versus the reciprocal of the 17OD concentration.

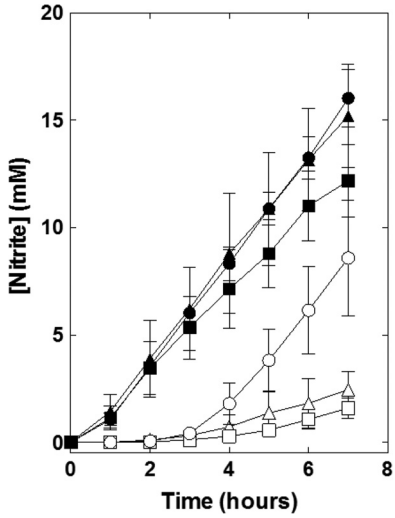

FIG 4 The time course of NH_4^+-dependent NO_2^- production for washed cells of *N. europaea* pretreated with or without 17OD, were determined, as described in the Materials and Methods section. The symbols are for incubations conducted with growth medium alone (● and ○), growth medium plus rifampin (100 μg ml^{-1}) (▲ and △), and growth medium plus chloramphenicol (400 μg ml^{-1}) (■ and □). The open symbols are for 17OD-treated cells, while the closed symbols are for untreated control cells. The plotted data show the mean and standard error of NO_2^- production for three biological replicates.

treated cells was strongly inhibited in incubations containing either rifampin or chloramphenicol. The maximal rate of NO_2^- production for 17OD-treated cells in the presence of these inhibitors was ≤20% of the rate observed in their absence. Substantially similar effects were previously observed during recovery of ammonia-oxidizing activity in *N. europaea* after its prior inactivation by acetylene (26). Our present results therefore suggest that 17OD is an irreversible inactivator of AMO and that recovery from the effects of this compound requires *de novo* protein synthesis.

CuAAC reaction with Alexa Fluor 647 azide. To test whether covalent modification of proteins could be detected by IR fluorescence, 17OD-pretreated cells were subjected to CuAAC reactions using Alexa Fluor 647 azide as a reporter as described in the Materials and Methods section. The cells were then solubilized in SDS-PAGE sample buffer and analyzed by SDS-PAGE and IR scanning. A single fluorescent 28-kDa polypeptide was observed for 17OD-pretreated cells reacted with Alexa Fluor 647 azide (16 μM) in the presence of $CuSO_4$ (2 mM), sodium ascorbate (11 mM), and THPTA (1 mM) (Fig. 5A, lane 3). No fluorescence was observed for cells if they had not previously been exposed to 17OD (Fig. 5A, lane 2) or if $CuSO_4$ (Fig. 5A, lane 4), sodium ascorbate (Fig. 5A, lane 5), or Alexa Fluor 647 azide (Fig. 5A, lane 6) was individually excluded from the CuAAC reactions.

In CuAAC reactions, $CuSO_4$ acts as the source of Cu^{1+} ions that catalyze the cycloaddition reaction. Ascorbate acts as a reductant that reduces Cu^{2+} to Cu^{1+} and that also reduces dissolved O_2. When added, THPTA acts as a ligand to stabilize Cu^{1+}. Along with aminoguanidine, THPTA also scavenges reaction by-products such as dehydroascorbate and reactive oxygen species that are generated during the conjugation reaction and that can react with and modify amino acids (35). Excluding THPTA from the CuAAC reactions conducted with whole cells slightly increased the level of fluorescent labeling of the 28-kDa polypeptide compared to that of reaction mixtures containing THPTA (Fig. 5A, lane 7). In the THPTA-free reaction, low levels of fluorescent labeling of an ~45-kDa polypeptide were also observed. In contrast, the addition of aminoguanidine had no discernible effect on the level of labeling of the 28-kDa polypeptide (Fig. 5A, lane 8). Similar results were obtained when frozen and lysed 17OD-treated cells were used in the CuAAC reactions (Fig. 5B). However, as was also suggested by our experiments shown in Fig. S1B, S2B, S3B, and S4B in the supplemental material, the labeling of the 28-kDa polypeptide was more intense when frozen, lysed cells were used compared to whole cells, but there was no discernible effect of using THPTA on the labeling reaction. Unless otherwise stated, the remainder of the CuAAC-labeling experiments reported in this study made use of intact whole cells with THPTA and aminoguanidine excluded from the CuAAC reaction.

To determine whether catalytically active AMO was required to observe fluorescent labeling of the 28-kDa polypeptide after exposure to 17OD, resting cells were incubated with and without allylthiourea (100 μM) prior to and during exposure to 17OD. After exposure to 17OD, the two cell samples were subjected to CuAAC reactions with Alexa Fluor 647 azide, solubilized in SDS-PAGE sample buffer and then analyzed by SDS-PAGE and IR scanning. The fluorescent 28-kDa polypeptide was detected in cells treated with 17OD alone (Fig. 6A, lane 4) but not in cells treated with allylthiourea prior to and during exposure to 17OD (Fig. 6A, lane 5). A similar effect was also observed if cells were treated with acetylene prior to exposure to 17OD. The 28-kDa polypeptide was detected in cells that had been treated with 17OD

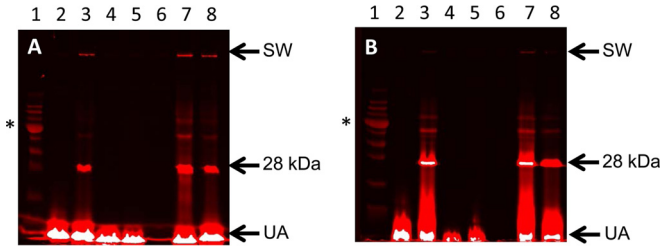

FIG 5 Intact 17OD-treated cells of *N. europaea* (A) or 17OD-treated cells that had been lysed by freezing (B) were reacted with Alexa Fluor 647 azide using a CuAAC reaction and analyzed by SDS-PAGE and IR scanning as described in the Materials and Methods section. In the two figures, the samples were as follows: lane 1, NIR markers; lane 2, cells without 17OD pretreatment reacted with $CuSO_4$ (2 mM), sodium ascorbate (11 mM), Alexa Fluor 647 azide (8 μM for frozen, lysed cells and 40 μM for whole cells), and THPTA (1 mM); lane 3, 17OD-pretreated cells reacted as for lane 2; lane 4, same as for lane 3 minus $CuSO_4$; lane 5, same as for lane 3 minus sodium ascorbate; lane 6, same as for lane 3 minus Alexa Fluor 647 azide; lane 7, same as for lane 3 minus TPHTA; lane 8, same as for lane 3 plus aminoguanidine (1 mM). SW, bottom of sample well; UA, unreacted Alexa Fluor 647 azide at gel dye front; *, 55-kDa marker protein.

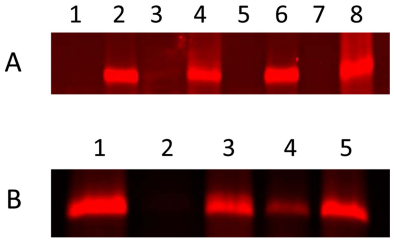

FIG 7 The IR fluorescence associated with the 28-kDa polypeptide in SDS-PAGE gel analyses of total protein from *N. europaea* was determined for cells pretreated with individual *n*-alkynes and diynes prior to the CuAAC-catalyzed reaction with Alexa Fluor 647 azide as described in the Materials and Methods section. (A) Cells were pretreated with the following: lane 1, 1-hexyne; lane 2, 1,5-hexadiyne; lane 3, 1-heptyne; lane 4, 1,6-heptadiyne; lane 5, 1-octyne; lane 6, 17OD; lane 7, 1-nonyne; lane 8, 1,8-nonadiyne. (B) Cells were pretreated with the following: lane 1, 17OD; lane 2, phenylacetylene; lane 3, 1,4-diethynylbenzene; lane 4, propargylamine; lane 5, dipropargylamine.

alone but was not detected in cells treated with acetylene alone or in cells treated with acetylene prior to exposure to 17OD (Fig. 6B).

To determine the cellular location of the fluorescent 28-kDa polypeptide, 17OD-treated cells were separated into crude soluble and particulate fractions by cycles of freezing and thawing followed by centrifugation. Samples of resulting fractions were reacted with Alexa Fluor 647 azide in CuAAC reactions and were then analyzed by SDS-PAGE and IR scanning. The fluorescent 28-kDa polypeptide was primarily detected in the membrane fraction when equivalent amounts of protein from the two fractions were analyzed (Fig. 6C).

To investigate whether the fluorescent 28-kDa polypeptide was susceptible to thermal- and reductant-dependent aggregation, samples of 17OD-pretreated cells were first reacted with Alexa Fluor 647 azide and were then solubilized in SDS-PAGE sample buffer using a variety of conditions. The resulting distribution of fluorescently labeled polypeptides was then determined by SDS-PAGE and IR analysis. For cells solubilized in SDS-PAGE sample buffer containing β-mercaptoethanol, the intensity of fluorescence associated with the 28-kDa polypeptide markedly decreased in samples heated at 95°C for 5 min (Fig. 6D, lane 4) compared to that of samples kept at room temperature (Fig. 6D, lane 2). In the sample heated at 95°C, there was also an increase in fluorescence associated with high-molecular-weight polypeptides. This aggregation effect was not as pronounced if the samples were first solubilized for 5 min at 95°C in an SDS-PAGE sample buffer that lacked β-mercaptoethanol (Fig. 6D, lane 3).

Fluorescent labeling after inactivation of AMO by *n*-alkynes and other diynes. Other potential diyne inactivators and their analogs with a single ethynyl functional group were investigated to determine whether they could be used to fluorescently label the 28-kDa polypeptide in *N. europaea*. In all cases, resting cells were first incubated with each alkyne or diyne (1 μmol) in the presence of NH_4Cl (10 mM). The amount of NO_2^- generated during the incubation was used to estimate the extent of inactivation of ammonia-oxidizing activity. After reaction with Alexa Fluor 647 azide in a CuAAC reaction and subsequent analysis by SDS-PAGE and IR scanning, a fluorescent 28-kDa polypeptide was observed for cells pretreated with 1,5-hexadiyne, 1,6-heptadiyne, 17OD, or 1,8-nonadiyne but not for cells pretreated with 1-hexyne, 1-heptyne, 1-octyne, or 1-nonyne (Fig. 7A). In all cases, NO_2^- production by cells during pretreatment with *n*-alkynes and diynes was inhibited by ≥95% compared to that of untreated control cells

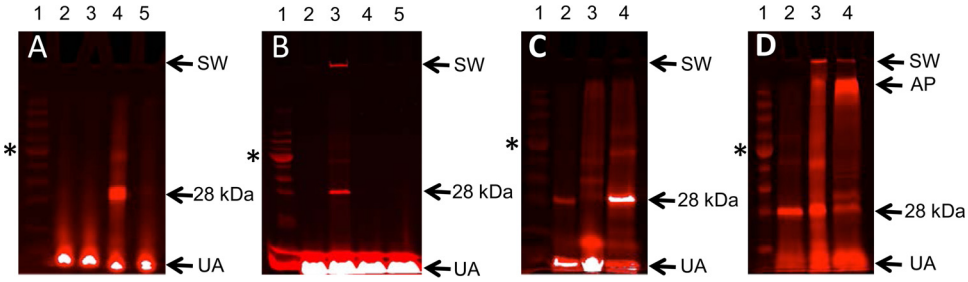

FIG 6 (A) Whole cells of *N. europaea* were (or were not) pretreated with 17OD in the presence and absence of allylthiourea, reacted with Alexa Fluor 647 azide, and analyzed by SDS-PAGE and IR scanning as described in the Materials and Methods section. Lane 1, NIR markers; lane 2, untreated cells (no 17OD); lane 3, untreated cells (no 17OD) plus allylthiourea; lane 4, 17OD-treated cells; lane 5, 17OD-treated cells plus allylthiourea. (B) Lane 1, NIR markers; lane 2, untreated cells (no 17OD); lane 3, 17OD-treated cells; lane 4, untreated cells (no 17OD) plus acetylene; lane 5, 17OD-treated cells plus acetylene. (C) Lane 1, NIR markers; lane 2, whole cells (25 μg protein); lane 3, soluble fraction (25 μg protein); lane 4, membrane fraction (25 μg protein). (D) Lane 1, NIR markers; lane 2, cells solubilized at room temperature in 2× SDS-PAGE sample buffer containing β-mercaptoethanol; lane 3, cells solubilized by heating for 5 min at 95°C in 2× SDS-PAGE sample buffer without β-mercaptoethanol; lane 4, cells solubilized by heating for 5 min at 95°C in 2× SDS-PAGE sample buffer containing β-mercaptoethanol. SW, bottom of sample well; AP, aggregated polypeptides; UA, unreacted Alexa Fluor 647 azide at gel dye front; *, 55-kDa marker protein.

(data not shown). Similarly, a fluorescent 28-kDa polypeptide was also observed for samples from cells pretreated with either dipropargylamine or 1,4-diethynylbenzene while little or no fluorescence was detected for cells pretreated with either propargylamine or phenylacetylene (Fig. 7B). The NH_4^+-dependent production of NO_2^- during the pretreatment of cells with phenylacetylene, 1,4-diethynylbenzene, and dipropargylamine was inhibited by ≥90% compared to that of untreated control cells, while cells pretreated with propargylamine generated ~35% of the amount of NO_2^- of untreated control cells (data not shown).

Mass spectral analyses of the 28-kDa polypeptide. Two approaches were used to identify the fluorescent 28-kDa polypeptide at the molecular level. In the first approach, the portion of an SDS-PAGE gel that contained the fluorescent 28-kDa polypeptide was excised and subjected to in-gel tryptic digestion followed by matrix-assisted laser desorption ionization–tandem time of flight (MALDI-TOF/TOF) analysis of the resulting peptide fragments. This analysis provided amino acid sequences for 6 distinct peptides. The most abundant of these peptides (45 hits) included 4 fragments that were all located within AmoA from *N. europaea* (see Fig. S5 in the supplemental material). The two remaining peptides (5 hits) were identified as fragments from the S3 30S ribosomal protein of *N. europaea*.

In the second approach, crude membrane fractions from 17OD-treated and control untreated cells were separately conjugated with biotin-azide using a CuAAC reaction and then affinity purified using streptavidin. After on-bead trypsin digestion of the purified proteins, the resulting peptide fragments were analyzed by liquid chromatography-mass spectrometry (LC-MS). To quantify the protein targets of the probe, the accurate mass and time (AMT) tag strategy was used to analyze the MS data. The AMT tag approach quantifies the area under the curve of each MS-identified peptide for a given protein. A rollup strategy is employed to determine a protein level abundance (36), which is based on the cumulative peptide quantification. The results of this analysis for the 20 most abundant proteins detected (Table 1) demonstrated that fragments from AmoA were the most frequently detected peptides for cell extracts treated with 17OD. In addition to AmoA, this analysis detected peptide fragments from other AMO components, and in combination, AmoA, AmoB, and AmoC were as much as 8-fold more abundant in 17OD-treated cell extracts than any other proteins detected. Other proteins, such as periplasmically located HAO and cytoplasmically located ribulose bisphosphate carboxylase/oxygenase (RUBISCO), were also detected as well as a native biotin-containing protein, the biotin carboxyl carrier protein of acetyl coenzyme A (CoA) carboxylase. The complete results from this AMT tag analysis for each detected protein are provided in Table S1 in the supplemental material.

DISCUSSION

Our results indicate that 17OD acts as a mechanism-based inactivator of AMO in *N. europaea*. Our results also indicate that 17OD and several other diynes can be used to detect catalytically active AMO using CuAAC conjugation and azide-containing tags suitable for fluorescent detection or affinity purification of the active-site-containing component (AmoA) of this enzyme. Many other bacterial monooxygenases are inactivated by alkynes, and the approach outlined in this study can potentially be used to detect, identify, and quantify other diyne-sensitive monooxygenases in complex samples. These main conclusions are discussed in more detail in the following sections.

Mechanism-based inactivation of AMO by 17OD. Establishing that a compound acts as a mechanism-based inactivator for a specific enzyme requires that the effects of the putative inactivator conform to a well-defined set of kinetic criteria (25). With purified enzymes, these criteria include, among others, an inactivator concentration-dependent, first-order loss of enzyme activity, the requirement for enzyme activity for inactivation to occur, and the irreversibility of the effects of the inactivator resulting from covalent modification of the enzyme (25). Our results obtained with whole cells illustrate that low concentrations of 17OD (≤10 μM) produced a concentration-dependent, first-order loss of NH_4^+-dependent O_2 uptake activity (Fig. 2 and 3). The effects of 17OD were apparently specific for AMO as 50 μM 17OD had no inhibitory effect on NH_2OH-dependent O_2 uptake (Fig. 2). Our conclusion that 17OD is an irreversible inactivator of AMO is supported by our observation that recovery of ammonia-oxidizing activity in 17OD-treated cells required *de novo* protein synthesis (Fig. 4).

With mechanism-based inactivators, true substrates for the target enzyme are expected to decrease the rate of inactivation due to competitive interactions between the substrate and the inactivator at the enzyme's active site (25). However, with some AMO inactivators studied in whole cells, NH_4^+ stimulates rather than decreases the rate of inactivation (21). This effect may reflect the need for concurrent ammonia oxidation to supply the reductant needed to support continued *in vivo* AMO activity. In this study, our experiments did not resolve an inhibitory or stimulating effect of NH_4^+ on the inactivation of NH_4^+-dependent NO_2^- production by 17OD, and a more detailed kinetic analysis will be required to clarify the role, if any, of NH_4^+ on this inactivation reaction. However, our measurements of NO_2^- production indicate that in all cases complete inactivation (≤99%) of AMO activity was observed for cells incubated with 17OD (1 μmol) and NH_4Cl (10 mM) under standardized conditions. Any variations in the subsequent CuAAC-dependent fluorescent labeling reported in this study therefore likely reflect the effects of variables associated with the CuAAC reaction itself rather than with the degree of prior inactivation of AMO.

Alexa Fluor 647 conjugation using CuAAC reactions. The results presented in this study consistently demonstrated that a CuAAC reaction using Alexa Fluor 647 azide and cells treated with either 17OD (Fig. 5, and 6) or a range of other diynes (Fig. 7) resulted in the fluorescent labeling of a membrane-associated 28-kDa polypeptide. Based on the precedent of ^{14}C labeling of AmoA in *N. europaea* after exposure to $^{14}C_2H_2$ (20, 26), we conclude that 17OD and other diynes target and inactivate AMO through catalytic activation of a terminal ethynyl group that results in the formation of a catalytically inactive, covalent enzyme-inactivator adduct (Fig. 1A). With diyne inactivators, this adduct retains a second unreacted terminal ethynyl group that can subsequently be conjugated with a fluorescent azide-containing reporter molecule, such as Alexa Fluor 647 azide (Fig. 1B). Conversely, the use of inactivators with only a single ethynyl group also resulted in inactivation of AMO but did not result in generation of a fluorescent product after CuAAC reactions (Fig. 7). This is presumably due to the lack of a second unreacted ethynyl group in the enzyme-inactivator adduct, which prevented subsequent CuAAC-dependent conjugation with Alexa Fluor 647 azide. Our observations that

TABLE 1 Quantitative proteomic analysis of probe (17OD) labeling of crude membrane fractions from *N. europaea*[a]

Locus tag(s)	Protein description	Probe mean[b]	Probe SD[c]	No probe mean[d]	No probe SD[e]	Fold difference[f]
ALW85_RS04940, ALW85_RS10750	AmoA, ammonia monooxygenase[g]	30.42	0.67	25.36	0.62	33.46
ALW85_RS04935, ALW85_RS10745	AmoB, ammonia monooxygenase[h]	29.75	0.57	22.79	0.12	124.37
ALW85_RS04945, ALW85_RS10755	AmoC, ammonia monooxygenase[i]	28.80	0.23	21.45	0.44	163.05
ALW85_RS05300	CoxB, cytochrome *c* oxidase polypeptide II precursor transmembrane protein	27.17	0.56	21.06	0.49	69.27
ALW85_RS10005	CbbL, ribulose bisphosphate carboxylase, large chain	26.75	0.47	20.53	0.27	74.16
ALW85_RS05030, ALW85_RS10645, ALW85_RS12195	Hao, hydroxylamine dehydrogenase[j]	26.37	0.28	20.14	0.09	69.78
ALW85_RS09655	Hypothetical protein	26.11	0.45	19.12	0.82	127.19
ALW85_RS03575	CoxB, possible cytochrome *c* oxidase chain II	25.70	0.67	18.80	0.93	119.20
ALW85_RS04925, ALW85_RS10735	Possible GenBank accession no. AF047705; unknown (*Nitrosococcus oceani*)[k]	25.57	0.20	19.33	0.11	75.38
ALW85_RS10075	Inorganic H^+ pyrophosphatase	25.41	0.56	19.83	0.37	47.86
ALW85_RS09995	CbbQ, nitric oxide reductase NorQ protein	25.39	0.31	19.42	0.21	62.71
ALW85_RS03415	AccB1, biotin carboxyl carrier protein of acetyl-CoA carboxylase	25.30	0.21	21.64	0.89	12.62
ALW85_RS13365	General diffusion Gram-negative porins	25.23	0.47	20.54	0.36	25.88
ALW85_RS04225	Rieske iron-sulfur protein 2Fe-2S subunit	25.13	0.29	18.79	0.24	81.20
ALW85_RS05020, ALW85_RS10635, ALW85_RS12185	CycA, cytochrome *c*-554 precursor[l]	24.65	0.35	19.09	0.08	46.99
ALW85_RS06890	IlvC, probable ketol-acid reductoisomerase oxidoreductase protein	24.46	0.05	19.45	0.02	32.30
ALW85_RS09670	Hypothetical protein	24.35	0.19	18.80	0.30	47.01
ALW85_RS10000	CbbS, ribulose bisphosphate carboxylase, small chain	24.34	0.09	18.03	0.59	79.06
ALW85_RS01135	Pal, bacterial outer membrane protein	24.29	0.11	19.76	0.74	23.02
ALW85_RS02050	60-kDa inner membrane protein	24.27	0.24	17.94	0.41	80.28

[a] See Table S1 in the supplemental material for additional data metrics and replicate data values.
[b] AMT tag data ($\log_2$ values) presented are the mean of three biological replicates of samples labeled with 17OD.
[c] Standard deviation (SD) of AMT tag quantitative data for samples labeled with 17OD.
[d] AMT tag data ($\log_2$ values) presented are the mean of two biological replicates of control samples treated with DMSO and no 17OD.
[e] SD of control samples treated with DMSO and no 17OD.
[f] Data presented are the magnitude of fold differences of protein abundances measured between 17OD-labeled and untreated samples. This shows clear protein labeling by 17OD and subsequent enrichment in 17OD-treated samples versus the untreated samples.
[g] Peptide amino acid sequences did not enable differentiation between ALW85_RS04940 and ALW85_RS10750.
[h] Peptide amino acid sequences did not enable differentiation between ALW85_RS04935 and ALW85_RS10745.
[i] Peptide amino acid sequences did not enable differentiation between ALW85_RS04945 and ALW85_RS10755.
[j] Peptide amino acid sequences did not enable differentiation between ALW85_RS05030, ALW85_RS10645, and ALW85_RS12195.
[k] Peptide amino acid sequences did not enable differentiation between ALW85_RS04925 and ALW85_RS10735.
[l] Peptide amino acid sequences did not enable differentiation between ALW85_RS05020, ALW85_RS10635, and ALW85_RS12185.

pretreatment of cells with either allylthiourea (Fig. 6A) or C_2H_2 (Fig. 6B) prior to exposure to 17OD subsequently prevented the fluorescent labeling of the 28-kDa polypeptide provide clear evidence that catalytic activity of AMO is required for 17OD to be effective as an ABPP probe for this enzyme.

It is important to note that we detected low levels of fluorescent labeling of the 28-kDa polypeptide in cells treated with propargylamine (Fig. 7B, lane 4). Based on the model outlined above, this is an unexpected result, as activation of the single ethynyl group of this compound by AMO leading to covalent modification of the enzyme would not be expected to leave an unreacted ethynyl group available for subsequent CuAAC conjugation reactions. As some propargylamine syntheses also produce di- and tri-propargylamine contaminants (37), this low-level fluorescent labeling may be due to the presence of these compounds in the commercially sourced propargylamine used in this study.

Our studies of key variables in the CuAAC-labeling reactions compared the same reactions using either whole cells or frozen, lysed cells (see Fig. S1 to S4 in the supplemental material). Overall, our results suggest that the CuAAC reaction proceeded faster with frozen, lysed cells than with intact cells (see Fig. S1) and that the Alexa Fluor 647 azide concentration was more critical in reactions with intact whole cells than with frozen, lysed cells (see Fig. S3). The simplest interpretation of these results is that Alexa Fluor 647 azide has limited permeability through the cell wall and membranes of intact cells. The effect of cell walls on the permeability of CuAAC reactants should be carefully considered in future applications of ABPP to microbial cells.

Protein analyses. Many of our observations concerning the fluorescently labeled 28-kDa polypeptide (Fig. 5 and 6) suggest that this polypeptide is AmoA, the same polypeptide previously shown to be radiolabeled when cells of *N. europaea* are incubated with $^{14}C_2H_2$ (20, 26). In this study, confirmation of the identity of this labeled polypeptide as AmoA was provided by two separate approaches. The most direct method involved MALDI-TOF/TOF analysis of the peptide fragments generated from an in-gel tryptic

digestion of the 28-kDa polypeptide (see Fig. S5 in the supplemental material). The less direct but potentially more versatile approach involved mass-spectral analysis of the proteolytic fragments of affinity-purified proteins from the crude membrane fraction of 17OD-treated cells (Table 1). This analysis also revealed that peptides from AmoA were the most abundant digestion fragments detected compared to control samples from cells that had not been exposed to 17OD. However, peptide fragments from other proteins were also detected, albeit at lower levels than AmoA. These peptides were either from highly abundant and metabolically important cytoplasmic (RUBISCO) or periplasmic enzymes (HAO) or other proteins directly associated with AMO (AmoB, AmoC) (5) or HAO (cytochrome c_{554}) (5). Some of these detections may have been due to adventitious binding of these abundant proteins to the streptavidin affinity purification matrix. However, it is also likely that this nonspecific detection is caused by diffusion of an activated form of 17OD away from its site of formation within AMO (27) and subsequent covalent modification of other proteins closely located to this enzyme in intact cells. Like AmoA, these additional proteins would be expected to retain an unreacted ethynyl group that would be available for reaction with biotin-azide in CuAAC reactions. These biotinylated proteins would then copurify with AmoA during streptavidin affinity purification and produce peptide fragments that can be identified by mass spectral analysis. For example, we observed a low level of fluorescent labeling of an ~45-kDa polypeptide in some of our analyses (Fig. 5), and our on-bead proteomic analysis (Table 1) suggests that this may be due to covalent modification of the 43-kDa AmoB polypeptide. Diffusion of an activated reactive inactivator away from the active site of AMO has previously been proposed to account for radiolabeling of proteins other than AmoA following inactivation of AMO by $^{14}C_2H_2$ (26) and is a common feature of mechanism-based inactivators (38).

Potential applications of ABPP. The ABPP approach described in this study is potentially applicable to many other alkyne-sensitive bacterial monooxygenases in pure cultures and complex microbial communities. While acetylene has been used to inactivate soluble and particulate methane monooxygenase (39) as well as propane-, butane-, toluene-, and tetrahydrofuran-oxidizing monooxygenases (40, 41), longer chain *n*-alkynes also inactivate several bacterial monooxygenases. For example, *n*-alkynes up to C_{10} inactivate AMO in *N. europaea* (11) and toluene-2-monooxygenase in *Burkholderia vietnamensis* G4 (42). Several *n*-alkynes, including 1-octyne, inactivate the alkene-oxidizing enzyme system of the 2-methylpropene metabolizing strain, *Mycobacterium* sp. ELW1 (43). The well-studied alkane hydroxylase in *Pseudomonas oleovorans* GPo1 is also irreversibly inactivated by 17OD (44–46).

The sensitivity of AMO to alkynes of differing carbon chain length has been the focus of recent studies of this enzyme in ammonia-oxidizing thaumarchaea (AOA). The AMOs in AOB and AOA are structurally similar but can be discriminated on the basis of their sensitivity to the concentration of *n*-alkyne mechanism-based inactivators, such as 1-ocytne (47, 48). The effects of *n*-alkynes on AMO in AOA conform to many of the kinetic criteria for mechanism-based inactivation. However, formation of covalent enzyme-inactivator adduct has not yet been established for *n*-alkyne-inactivated AMO in AOA. Although 17OD may be an effective probe for AMO in AOA, this enzyme is most sensitive to inactivation by shorter chain *n*-alkynes ($<C_6$), and terminal diynes smaller than 1,5-hexadiyne are reactive and are difficult to prepare or obtain commercially. Another potential probe suggested by this study is phenylacetylene and its diyne analog 1,4-diethynylbenzene. Phenylacetylene is a mechanism-based inactivator for AMO in *N. europaea* (20). It would be interesting to determine whether AMO in AOA is sensitive to these inactivators and whether, like AMO in *N. europaea*, AMO in AOA can be detected using 1,4-diethynylbenzene as an ABPP probe.

The ABPP approach described here may also potentially be applied to detect, identify, and quantify catalytically active diyne-sensitive bacterial monooxygenases in complex microbial communities and environmental samples. In particular, using ABPP to affinity purify biotin-labeled enzyme-inactivator adducts has the potential to greatly reduce the complexity of protein samples obtained from these sources. Covalent fluorescent labeling of active monooxygenases in whole cells may also be exploited in fluorescence microscopy, flow cytometry, and fluorescence-activated cell sorting. Our current research is exploring the range of bacterial monooxygenases that are susceptible to inactivation by diynes and detection by ABPP as well as developing methods to detect these enzymes and microorganisms harboring these enzymes in environmental samples.

ACKNOWLEDGMENTS

We thank Nedyalka Dicheva at the University of North Carolina—Chapel Hill Proteomics Center for conducting the in gel digestion and MALDI-TOF/TOF analyses. A portion of the research was also performed using EMSL, a DOE Office of Science User Facility sponsored by the Office of Biological and Environmental Research (OBER) located at Pacific Northwest National Laboratory.

A.T.W. and N.C.S. were supported in part by the Pan-omics project, a part of the Genomic Science Program of the OBER.

FUNDING INFORMATION

Strategic Environmental Research and Development Program provided funding to Michael R. Hyman under grant number ER2302.

REFERENCES

1. **Speers AE, Adam GC, Cravatt BF.** 2003. Activity-based protein profiling *in vivo* using a copper(I)-catalyzed azide-alkyne [3 + 2] cycloaddition. J Am Chem Soc **125:**4686–4687. http://dx.doi.org/10.1021/ja034490h.
2. **Barglow KT, Cravatt BF.** 2007. Activity-based protein profiling for the functional annotation of enzymes. Nat Methods **4:**822–827. http://dx.doi.org/10.1038/nmeth1092.
3. **Sadler NC, Wright AT.** 2015. Activity-based protein profiling of microbes. Curr Opin Chem Biol **24:**139–144. http://dx.doi.org/10.1016/j.cbpa.2014.10.022.
4. **Wright AT, Cravatt BF.** 2007. Chemical proteomic probes for profiling cytochrome P450 activities and drug interactions *in vivo*. Chem Biol **14:**1043–1051. http://dx.doi.org/10.1016/j.chembiol.2007.08.008.
5. **Arp DJ, Stein LY.** 2003. Metabolism of inorganic N compounds by ammonia-oxidizing bacteria. Crit Rev Biochem Mol Biol **38:**471–495. http://dx.doi.org/10.1080/10409230390267446.
6. **Ensign SA, Hyman MR, Arp DJ.** 1993. *In vitro* activation of ammonia monooxygenase from *Nitrosomonas europaea* by copper. J Bacteriol **175:**1971–1980.
7. **Juliette LY, Hyman MR, Arp DJ.** 1995. Roles of bovine serum albumin and copper in assays and stability of ammonia monooxygenase activity *in vitro*. J Bacteriol **177:**4908–4913.
8. **Gilch S, Meyer O, Schmidt I.** 2010. Electron paramagnetic studies of the copper and iron containing soluble ammonia monooxygenase from *Nitrosomonas europaea*. Biometals **23:**613–622. http://dx.doi.org/10.1007/s10534-010-9308-2.
9. **Bedard C, Knowles R.** 1989. Physiology, biochemistry, and specific inhibitors of CH_4, NH_4^+, and CO oxidation by methanotrophs and nitrifiers. Microbiol Rev **53:**68–84.

10. **Hyman M, Wood PM.** 1983. Methane oxidation by *Nitrosomonas europaea*. Biochem J **212:**31–37. http://dx.doi.org/10.1042/bj2120031.
11. **Hyman MR, Murton IB, Arp DJ.** 1988. Interaction of ammonia monooxygenase from *Nitrosomonas europaea* with alkanes, alkenes, and alkynes. Appl Environ Microbiol **54:**3187–3190.
12. **Hyman MR, Wood PM.** 1984. Ethylene oxidation by *Nitrosomonas europaea*. Arch Microbiol **137:**155–158. http://dx.doi.org/10.1007/BF00414458.
13. **Hyman MR, Sanesome-Smith AW, Wood PM.** 1985. A kinetic study of benzene oxidation to phenol by whole cells of *Nitrosomonas europaea* and evidence for the further oxidation of phenol to hydroquinone. Arch Microbiol **143:**302–306. http://dx.doi.org/10.1007/BF00411254.
14. **Keener WK, Arp DJ.** 1994. Transformations of aromatic compounds by *Nitrosomonas europaea*. Appl Environ Microbiol **60:**1914–1920.
15. **Hyman MR, Page CL, Arp DJ.** 1994. Oxidation of methyl fluoride and dimethyl ether by ammonia monooxygenase in *Nitrosomonas europaea*. Appl Environ Microbiol **60:**3033–3035.
16. **Juliette LY, Hyman MR, Arp DJ.** 1993. Inhibition of ammonia oxidation by sulfur compounds: thioethers are oxidized to sulfoxides by ammonia monooxygenase. Appl Environ Microbiol **59:**3718–3727.
17. **Vannelli T, Logan M, Arciero D, Hooper AB.** 1990. Degradation of halogenated aliphatics by the ammonia-oxidizing bacterium *Nitrosomonas europaea*. Appl Environ Microbiol **56:**1169–1171.
18. **Rasche ME, Hicks RE, Hyman MR, Arp DJ.** 1990. Oxidation of monohalogenated ethanes and *n*-chlorinated alkanes by whole cells of *Nitrosomonas europaea*. J Bacteriol **172:**5368–5373.
19. **Keener WK, Arp DJ.** 1993. Kinetic studies of ammonia monooxygenase inhibition in *Nitrosomonas europaea* by hydrocarbons and halogenated hydrocarbons in an optimized whole-cell assay. Appl Environ Microbiol **59:**2501–2510.
20. **Hyman MR, Wood PM.** 1985. Suicidal inactivation and labelling of ammonia mono-oxygenase by acetylene. Biochem J **227:**719–725. http://dx.doi.org/10.1042/bj2270719.
21. **Keener WK, Russell SA, Arp DJ.** 1998. Kinetic characterization of the inactivation of ammonia monooxygenase in *Nitrosomonas europaea* by alkyne, aniline and cyclopropane derivatives. Biochim Biophys Acta **1388:**373–385. http://dx.doi.org/10.1016/S0167-4838(98)00188-5.
22. **Juliette LY, Hyman MR, Arp DJ.** 1993. Mechanism-based inactivation of ammonia monooxygenase in *Nitrosomonas europaea* by allylsulfide. Appl Environ Microbiol **59:**3728–3735.
23. **Hynes RK, Knowles R.** 1978. Inhibition by acetylene of ammonia oxidation in *Nitrosomonas europaea*. FEMS Microbiol Lett **4:**319–321. http://dx.doi.org/10.1111/j.1574-6968.1978.tb02889.x.
24. **Hynes RK, Knowles R.** 1982. Effect of acetylene on autotrophic and heterotrophic nitrification. Can J Microbiol **28:**334–340. http://dx.doi.org/10.1139/m82-049.
25. **Abeles RH, Maycock AL.** 1976. Suicide enzyme inactivators. Acc Chem Res **9:**313–319. http://dx.doi.org/10.1021/ar50105a001.
26. **Hyman MR, Arp DJ.** 1992. $^{14}C_2H_2$- and $^{14}CO_2$-labeling studies of the *de novo* synthesis of polypeptides by *Nitrosomonas europaea* during recovery from acetylene and light inactivation of ammonia monooxygenase. J Biol Chem **267:**1534–1545.
27. **Gilch S, Vogel M, Lorenz MW, Meyer O, Schmidt I.** 2009. Interaction of the mechanism-based inactivator acetylene with ammonia monooxygenase of *Nitrosomonas europaea*. Microbiology **155:**279–284. http://dx.doi.org/10.1099/mic.0.023721-0.
28. **McTavish H, Fuchs JA, Hooper AB.** 1993. Sequence of the gene coding for ammonia monooxygenase in *Nitrosomonas europaea*. J Bacteriol **175:**2436–2444.
29. **Hommes NG, Sayavedra-Soto LA, Arp DJ.** 1998. Mutagenesis and expression of *amo*, which codes for ammonia monooxygenase in *Nitrosomonas europaea*. J Bacteriol **180:**3353–3359.
30. **Sagné C, Isambert M-F, Henery J-P, Gasnier B.** 1996. SDS-resistant aggregation of membrane proteins: application to the purification of the vesicular monoamine transporter. Biochem J **316:**825–831. http://dx.doi.org/10.1042/bj3160825.
31. **Rath A, Glibowicka M, Nadeau VG, Chen G, Deber CM.** 2009. Detergent binding explains anomalous SDS-PAGE migration of membrane proteins. Proc Nat Acad Sci U S A **106:**1760–1765. http://dx.doi.org/10.1073/pnas.0813167106.
32. **Hyman MR, Arp DJ.** 1993. An electrophoretic study of the thermal- and reductant-dependent aggregation of the 27 kDa component of ammonia monooxygenase from *Nitrosomonas europaea*. Electrophoresis **14:**619–627. http://dx.doi.org/10.1002/elps.1150140197.
33. **Hageman RH, Huckleby DP.** 1971. Nitrate reductase from higher plants. Methods Enzymol **23:**491–503. http://dx.doi.org/10.1016/S0076-6879(71)23121-9.
34. **Gornall AG, Bardawill CJ, David MM.** 1949. Determination of serum proteins by means of the biuret reaction. J Biol Chem **177:**751–766.
35. **Hong V, Presolski SI, Ma C, Finn MG.** 2009. Analysis and optimization of copper-catalyzed azide-alkyne cycloaddition for bioconjugation. Angew Chem Int Ed Engl **48:**9879–9883. http://dx.doi.org/10.1002/anie.200905087.
36. **Polpitiya AD, Qian W-J, Jaitly N, Petyuk VA, Adkins JN, Camp DG, II, Anderson GA, Smith RD.** 2008. DAnTE: a statistical tool for quantitative analysis of -omics data. Bioinformatics **24:**1556–1558. http://dx.doi.org/10.1093/bioinformatics/btn217.
37. **Seko S, Nakamura A, Hazama M.** May 1998. Method for producing propargylamine compounds. US patent 5,756,769.
38. **Siverman RB.** 1995. Mechanism-based enzyme inactivators. Methods Enzymol **249:**331–370.
39. **Prior S, Dalton H.** 1985. Acetylene as a suicide substrate and active site probe for methane monooxygenase from *Methylococcus capsulatus* (Bath). FEMS Microbiol Lett **29:**105–109. http://dx.doi.org/10.1111/j.1574-6968.1985.tb00843.x.
40. **Mahendra S, Alvarez-Cohen L.** 2006. Kinetics of 1,4-dioxane biodegradation by monooxygenase-expressing bacteria. Environ Sci Technol **40:**5435–5442. http://dx.doi.org/10.1021/es060714v.
41. **Hanamura N, Storfa RT, Semprini L, Arp DJ.** 1999. Diversity in butane monooxygenases among butane-grown bacteria. Appl Environ Microbiol **65:**4586–4593.
42. **Yeager CM, Bottomley PJ, Arp DJ, Hyman MR.** 1999. Inactivation of toluene-2-monooxygenase in *Burkholderia cepacia* G4 by alkynes. Appl Environ Microbiol **65:**632–639.
43. **Kottegoda S, Waligora E, Hyman M.** 2015. Metabolism of 2-methylpropene (isobutylene) by the aerobic bacterium *Mycobacterium* sp. strain ELW1. Appl Environ Microbiol **81:**1966–1976. http://dx.doi.org/10.1128/AEM.03103-14.
44. **May SW, Katapodis AG.** 1986. Oxygenation of alcohol and sulfide substrates by a prototypical non-haem iron monooxygenase: catalysis and biotechnological potential. Enzyme Microb Technol **8:**17–21. http://dx.doi.org/10.1016/0141-0229(86)90004-9.
45. **May SW, Svchwartz RD, Abbott BJ, Zaborsky OR.** 1975. Structural effects on the reactivity of substrates and inhibitors in the epoxidation system of *Pseudomonas oleovorans*. Biochim Biophys Acta **403:**245–255. http://dx.doi.org/10.1016/0005-2744(75)90026-1.
46. **Smith CA, Hyman MR.** 2004. Oxidation of methyl *tert*-butyl ether by alkane hydroxylase in dicyclopropylketone-induced and *n*-octane-grown *Pseudomonas putida* GPo1. Appl Environ Microbiol **70:**4544–4550. http://dx.doi.org/10.1128/AEM.70.8.4544-4550.2004.
47. **Taylor AE, Vajrala N, Giguere AT, Gitelman AI, Arp DJ, Myrold DD, Sayavedra-Soto L, Bottomley PJ.** 2013. Use of aliphatic *n*-alkynes to discriminate soil nitrification activities of ammonia-oxidizing thaumarchaea and bacteria. Appl Environ Microbiol **79:**6544–6551. http://dx.doi.org/10.1128/AEM.01928-13.
48. **Taylor AE, Taylor K, Tennigkeit B, Palatinszky M, Stiegmeier M, Myrold DD, Schleper C, Wagner M, Bottomley PJ.** 2015. Inhibitory effects of C_2 to C_{10} 1-alkynes on ammonia oxidation by two *Nitrosophaera* species. Appl Environ Microbiol **81:**1942–1948. http://dx.doi.org/10.1128/AEM.03688-14.